Hindawi
Adsorption Science & Technology
Volume 2023, Article ID 6695937, 12 pages
https://doi.org/10.1155/2023/6695937

Research Article

Malachite Green Removal by Grape Stalks Biosorption from Natural Waters and Effluents

Eliana S. Lemos,[1] Emiliano F. Fiorentini,[1] Adrián Bonilla-Petriciolet,[2] and Leticia B. Escudero[1]

[1]*Laboratory of Environmental Biotechnology (BioTA), Interdisciplinary Institute of Basic Sciences (ICB), UNCUYO-CONICET, Faculty of Natural and Exact Sciences, National University of Cuyo, Padre Contreras 1300, (5500) Mendoza, Argentina*
[2]*Chemical Engineering Department, Instituto Tecnológico de Aguascalientes, Aguascalientes 20256, Mexico*

Correspondence should be addressed to Leticia B. Escudero; letibelescudero@gmail.com

Received 31 January 2023; Revised 14 March 2023; Accepted 28 March 2023; Published 14 June 2023

Academic Editor: Lingzhi Yang

The efficiency of the grape stalk as a biosorbent for the malachite green removal from natural waters and industrial effluents was investigated in this work. For the optimization of experimental variables, a central composite design was used, in which the effect of pH and biosorbent dose was evaluated on biosorption capacity and removal percentage. Optimal parameters of pH 5 and biosorbent dose of 0.80 g L^{-1} allowed a malachite green removal percentage of 87.7%. Data obtained from kinetic studies were fitted with the pseudo-second-order model. The maximum biosorption capacity was determined using the Langmuir equilibrium model, reaching a value of 214.2 mg g^{-1}. The biosorption process was thermodynamically favorable and spontaneous at room temperature. The calculated value of biosorption enthalpy change indicated that the nature of the process was exothermic and physical. The biosorption process was applied in natural waters and industrial effluent samples, obtaining removal percentages up to 84.3%, which demonstrates the efficiency of grape stalks for the treatment of complex matrices.

1. Introduction

One of the main activities that plays an important role in the economy of many countries is derived from the textile industry [1, 2]. This industry is considered one of the largest generators of wastewater because it uses significant volumes of fresh water in all production stages. In fact, it has been reported that approximately 200 L of water is used on average to make 1 kg of textiles [3–5]. The wastewater generated by the textile industry contains a large amount of colored compounds and toxic chemical products that can cause serious damage to the health of living beings if they are discharged into the environment without prior decontamination treatment [1, 2]. The presence of synthetic dyes in effluents represents a serious environmental problem because they are not biodegradable under natural conditions [6, 7].

Malachite green (MG) or 4{[4-(dimethylamino)phenyl](phenyl)methylidene}-N,N-dimethylcyclohexa-2,5-dien-1-iminium chloride is a synthetic cationic dye of diaminotriphenylmethane N-methylated [8]. This organic compound is used in the textile industry for dyeing wool, cotton, and silk, in the tannery for dyeing leather; in the paper industry, ceramics; and in aquaculture as a bactericide, fungicide, and parasiticide [9]. The presence of MG in the environment represents a risk to human health, since it is considered a multiorgan toxin, and its toxicity increases with exposure time, temperature, and concentration [10–12]. This dye can enter to the food chain via contaminated water or contaminated fish, shrimp, and crabs, causing effects on human health such as skin, gastrointestinal, and respiratory irritation. It can also cause carcinogenesis, mutagenesis, and teratogenesis [13–16]. Taking into account the previous aspects, studies focused on the development of technologies

for the MG removal from contaminated matrices are of great relevance, not only for the preservation of public health but also for the environmental protection.

In recent years, different treatment technologies have been used to remove MG from aqueous solutions, natural waters, and/or industrial effluents, including biological processes [17], chemical methods such as oxidation [18], and physical treatments including the use of membranes [19]. Although these treatments have been widely used for the removal of toxic dyes from contaminated sites, they generally have the limitation of being expensive, requiring high energy expenditure, and producing concentrated sludge. As a promising alternative, adsorption arises for its effectiveness and cost-effective characteristics, which have been exploited using different solid phases [20–23]. In this sense, biosorption has been highlighted in recent years to reduce textile dye concentrations from contaminated matrices through a low-cost and environmentally friendly way [24], using raw materials available in nature that do not require complex processing prior to their use [25].

Within the great variety of biosorbents, plant residues have allowed the development of a wide range of dye removal processes, which have the advantages of low cost, high abundance, and generating few by-products [25, 26]. Although it has been reported the use of grapevine plant components as biosorbents for some pollutants [27, 28], further contributions are desirable to study additional pollutant/plant biosorbent systems for the decontamination of real samples. In this way, the novelty of this work was focused on the use of the grape stalk as a biosorbent for the removal of MG from natural water samples and industrial effluents. The grape stalk was selected as a biosorbent material considering that it is a component of the vine plant and also a residue from the wine industry, which makes it an economical, easy-to-obtain, abundant, and alternative material to be used in water cleaning. Thus, the objective of this work was to test and characterize the performance of a novel, efficient, economical, and environmentally friendly laboratory-scale biosorption process that allows the malachite green removal from natural water and industrial effluent samples using grape stalks. The optimization, kinetic, and thermodynamic studies were performed to evaluate the MG biosorption process. To the best of our knowledge, this is the first time that grape stalk has been used as a biosorbent for the removal of MG from aqueous environmental samples.

2. Materials and Methods

2.1. Biosorbent Preparation. The grape stalks (*Vitis vinifera*) were obtained in Mendoza province, Argentina. The biosorbent was prepared by manually selecting the stalks, washing them with tap water, and then rinsing them with distilled water. The stalks were lyophilized (VirTis Freezemobile, Model 6, USA), and the material was pulverized using a mill (Ultracomb, MO-8100A, Argentina) and sieved to obtain a homogeneous particle size from 80 to 106 μm and a BET surface area of 0.42 $m^2 g^{-1}$. These grape stalks were used for subsequent experiments.

2.2. Characterization Techniques. To study the charge on the biosorbent surface at the working pH, the pH of the point of zero charge (pH_{pzc}) was determined by adapting a procedure previously reported in the literature [29]. Erlenmeyer flasks containing 50 mL of NaCl solution with a concentration of 0.01 mol L^{-1} were used. The pH of each solution was adjusted from 2 to 12, using solutions of 0.1 mol L^{-1} HCl and 0.1 mol L^{-1} NaOH. Then, 150 mg of biosorbent was added and subjected to thermostatic agitation (Arcano SHZ-88, China) for 24 h at 298 K. After this time, the final pH of each solution was measured. The pH_{pzc} was obtained by intersecting the curve of final and initial pH.

The functional groups present on the biosorbent surface were characterized before and after the biosorption process by Fourier transform infrared spectroscopy (FT-IR) (PerkinElmer, Spectrum Two) under the attenuated total reflectance (ATR) mode. FT-IR spectra were analyzed in a wavenumber range of 4000 to 400 cm^{-1}.

In addition, the scanning electron microscope (SEM) (JEOL, JSM-6610LV, Japan) was used to evaluate the surface morphology of grape stalks before and after the biosorption process. To perform the scanning, the samples were spread on 12 mm diameter PELCO carbon stubs with a bifaced conductive tape in the *X*-, *Y*-, and *Z*-axes. They were covered with gold and observed by SEM at 5 kV, and the working distance (WD) was 11 mm.

2.3. Reagents and Solutions. Malachite green dye (4{[4-(dimethylamino)phenyl](phenyl)methylidene}-N,N-dimethylcyclohexa-2,5-dien-1-iminium chloride; CI 42000; molecular formula $C_{23}H_{25}ClN_2$; molecular weight 364.91 g mol^{-1}; λ_{max} = 619 nm) came from Vetec (Brazil). A standard dye stock solution with a concentration of 1000 mg L^{-1} was prepared, and dilutions were made with distilled water. To adjust the pH of each solution, a pH meter (Apera Instruments, PC910, China) and 0.1 mol L^{-1} NaOH and HCl solutions were used.

2.4. Biosorption Experiments. The biosorption experiments were performed in a batch system, placing firstly 25 mL of MG solution with a concentration of 50 mg L^{-1} in Erlenmeyer flasks. The pH of each solution was adjusted to 3, 5, and 7. Then, 20, 40, or 60 mg of biosorbent were added to the MG solutions. The Erlenmeyer flasks were placed under thermostatic agitation at 140 rpm for 120 min at room temperature. After that, the solid phase was separated from the aqueous phase by centrifugation at 3000 rpm for 5 min. Blank adsorption experiments were also performed without the biosorbent to check that no dye molecule was adsorbed on the wall of the Erlenmeyer flasks.

Kinetic studies were performed once the optimal conditions of biosorption experiments were determined. In these experiments, 25 mL of MG solutions with initial concentrations of 50 and 100 mg L^{-1} was utilized. The pH was adjusted to 5, and 20 mg of biosorbent was added to each solution. The Erlenmeyer flasks were placed under agitation with a stirring speed of 140 rpm at room temperature, and different contact times ranging from 0 to 180 min were evaluated.

After that, the phases were separated by centrifugation at 3000 rpm for 5 min.

For the equilibrium assays, dye solutions were prepared at initial concentrations of 25, 50, 100, 150, 200, and 300 mg L^{-1}. Solutions were adjusted to optimum pH, and 20 mg of biosorbent was added to each Erlenmeyer flask, which was placed under agitation for 120 min at temperatures of 298, 308, 318, and 328 K. Finally, a centrifugation step at 3000 rpm for 5 min was performed to separate the solid phase from the aqueous solution.

The MG concentration was determined in all the aforementioned experiments in the aqueous phase obtained after centrifugation by UV-Vis spectrophotometry (Shimadzu, UV-1800), at the maximum wavelength (616 nm). Calibration was performed with blank solutions and standard aqueous solutions.

The percent dye removal (%R) was calculated using Equation (1) and the biosorption capacity, q_t (mg g^{-1}), at time t was determined by Equation (2):

$$R = \frac{(C_0 - C_e)}{C_0} \times 100, \quad (1)$$

$$q_t = \frac{V(C_0 - C_t)}{m}, \quad (2)$$

where C_0, C_e, and C_t (mg L^{-1}) are dye concentrations in the liquid phase at the initial, equilibrium, and any time t, respectively. V (L) is the solution volume, and m (g) is the biosorbent mass.

2.5. Multivariate Optimization of Removal Conditions. The optimization of the experimental variables considered important in the biosorption process (pH and biosorbent dose) was performed using a central composite design centered on faces 3^2, where the biosorption capacity and the removal percentage were represented as a function of the pH (3, 5, and 7) and the dose of biosorbent (0.80, 1.60, and 2.50 g L^{-1}). The adsorption capacity and dye removal were expressed with the following equation:

$$q = a + \sum_{i=1}^{n} b_i x_i + \sum_{i=1}^{n} b_{ii} x_i^2 + \sum_{i=1}^{n-1} \sum_{j=i+1}^{n} b_{ij} x_i x_j, \quad (3)$$

where "a" is the constant coefficient, "b_i" is the linear coefficients, "b_{ij}" is the interaction coefficients, "b_{ii}" is the quadratic coefficients, and "x_i" and "x_j" are the coded values of the variables [30]. The statistical significance of nonlinear regression was evaluated by analysis of variance (ANOVA), and the quadratic polynomial equation of the model was evaluated by Fisher's test. The results obtained were analyzed using the software STASTISTICA 9.1 (StatSoft Inc., USA).

2.6. Kinetic and Isothermal Models. For a better understanding of the biosorption process, pseudo-first-order (PFO) and pseudo-second-order (PSO) kinetic models were assessed. Regarding equilibrium biosorption, the experimental data were fitted to the Langmuir and Freundlich isotherm models [31, 32]. The equations are detailed in Supplementary material 1.

2.7. Thermodynamic Studies. The values of the standard Gibbs free energy change ($\Delta G\circ$, kJ mol^{-1}), enthalpy change ($\Delta H\circ$, kJ mol^{-1}), and entropy change ($\Delta S\circ$, kJ mol^{-1}) were estimated as it is explained in Supplementary material 2 [33].

2.8. Modeling and Estimation of Parameters. The kinetic parameters and adsorption isotherms were determined by nonlinear regression using the software STATISTICA 9.1. Fitting quality was measured according to the determination coefficient (R^2), Fisher's test (F), and the average relative error (ARE) where these values were calculated as it is described in Supplementary material 3 [34].

2.9. Application of Grape Stalk Biosorbent to Real Samples. The natural water samples were collected in different sectors of the region and extracted as aliquots in labeled, clean, and dry containers. The seawater sample came from Chile, the river water sample came from San Luis (Argentina), and the dam and well water samples came from the Potrerillos Dam and Corralitos town in Mendoza (Argentina).

The agricultural effluent was provided by the Bromatological Laboratory of Junín (Mendoza, Argentina), and the textile effluent was obtained from a jeans factory. The effluents were collected in clean containers and kept at low temperatures.

Moreover, a synthetic textile effluent (pH 5) was prepared considering a previously described procedure [35], which contained the following components: $CaSO_4$ (130 mg L^{-1}), $CaCl_2$ (312 mg L^{-1}), $NaHCO_3$ (520 mg L^{-1}), $MgSO_4$ (316 mg L^{-1}), crystal violet (5 mg L^{-1}), and methylene blue (1 mg L^{-1}). All samples were prepared by placing 25 mL in Erlenmeyer flasks and adding MG concentrations of 25 and 50 mg L^{-1}. The pH was adjusted to the optimum value, and 20 mg of stalks was added. The solutions were stirred for 120 min at room temperature, with a stirring speed of 140 rpm. Then, the solid phase was separated from the aqueous phase by centrifugation at 3000 rpm for 5 min. The concentration of MG in the supernatant was determined by UV-Vis spectrophotometry before and after the biosorption process.

3. Results and Discussion

3.1. Biomaterial Characterization. The biosorbent was characterized by pH_{pzc}, FTIR, and SEM. The pH_{pzc} of the biosorbent was 4.5 (Figure 1). This pH_{pzc} value indicates that the surface of the grape stalk stem is negatively charged at pH values > 4.5, while the biosorbent surface is positively charged at pH values < 4.5 [36]. Therefore, it is expected that the grape stalk-MG system will be favored at pH levels higher than the pH_{pzc}, due to the dye molecules that are positively charged.

Figure 2 shows the FTIR spectra obtained for the grape stalk before and after the biosorption process. In the spectrum of stalk grape obtained before the biosorption process, the characteristic absorption band of the plant-derived biosorbent could be observed at 3277 cm^{-1}, which is due to the stretching of the O-H and N-H bonds. On the other hand, the absorption bands of stretching of C-H groups in

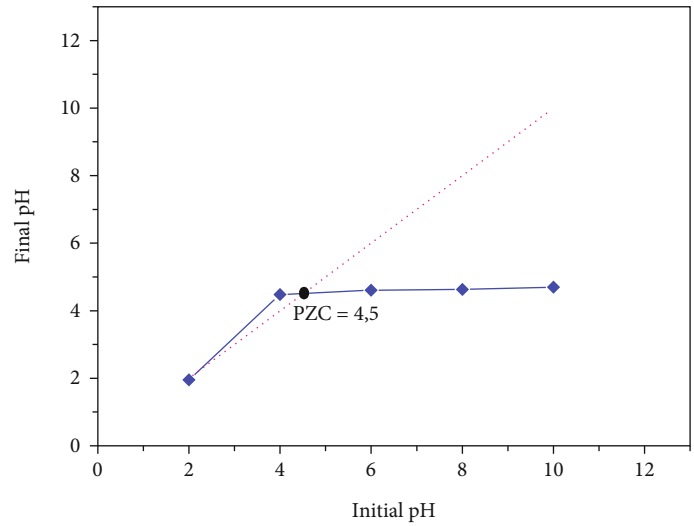

Figure 1: Point of zero charge obtained for the grape stalk.

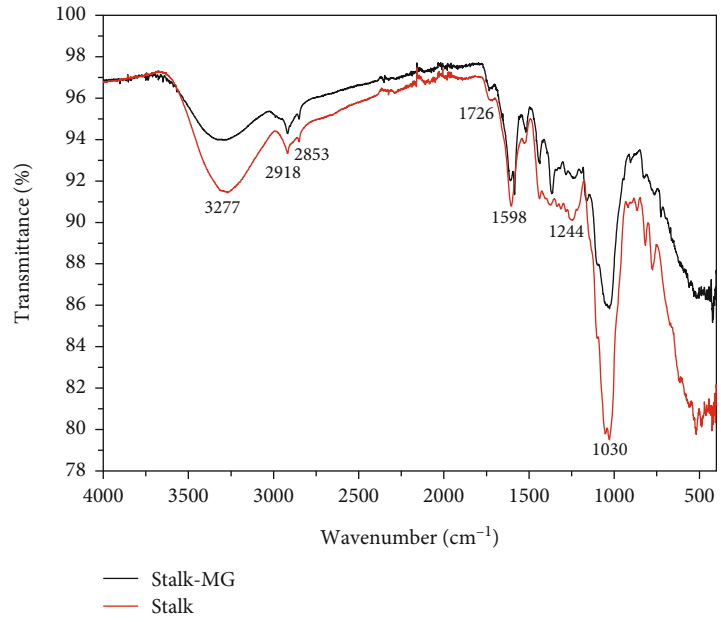

Figure 2: FTIR spectra of grape stalk (red line) and grape stalk with adsorbed MG (black line).

olefinic chains can be seen at 2918 and 2853 cm^{-1} [37]. The signal at 1726 cm^{-1} could correspond to the absorption of ester-type carbonyl groups and the band at 1598 cm^{-1} to vibrations coming from an aromatic nucleus. Finally, the absorption band of the aromatic type vibrations of C-O groups was observed at 1030 cm^{-1}, which is a characteristic of the lignin structure present in the grape stalk [38, 39]. After the biosorption process (MG-stalk), some absorption band shifts corresponding to O-H and N-H stretches were observed, which could suggest that the dye was adsorbed on the surface of the biosorbent through the O-H and N-H groups as adsorption sites [40]. The absorption band shifts at 1040, 1581, and 1363 cm^{-1} were also observed, indicating that the aromatic C-O, C=C, and C-N groups could be involved in the biosorption process.

SEM micrographs of the grape stalk were obtained before and after the biosorption process (Figure 3). Before the biosorption process, roughness and heterogeneity were observed on the surface of the grape stalks (Figure 3(a)). After the dye adsorption, changes were observed on the stalk surface, presenting smoothness and softness, being able to conclude that the grape stalk adsorbed the MG dye on its surface (Figure 3(b)).

3.2. Experimental Design for the Optimization of Malachite Green Biosorption. The experimental design matrix and the results obtained through the use of a central composite design centered on faces 3^2 can be seen in Table 1. It can be observed that the MG removal percentages were high for all the tested pH values and biosorbent doses. These

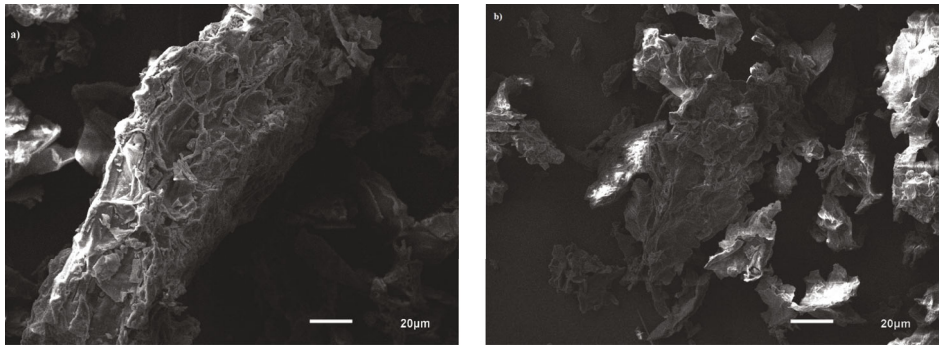

Figure 3: SEM micrographs of (a) grape stalk and (b) grape stalk with adsorbed MG.

Table 1: Experimental design matrix and results for MG biosorption by grape stalk.

Experiment	pH [coded form]	Biosorbent dosage ($g\,L^{-1}$) [coded form]	R (%)[a]	q ($mg\,g^{-1}$)
1	3 [−1]	0.80 [−1]	84.6 ± 3.0	52.1 ± 2.5
2	3 [−1]	1.60 [0]	91.2 ± 3.1	28.5 ± 1.4
3	3 [−1]	2.40 [+1]	96.0 ± 3.2	20.0 ± 1.3
4	5 [0]	0.80 [−1]	87.7 ± 3.0	54.8 ± 2.4
5	5 [0]	1.60 [0]	95.3 ± 3.2	29.8 ± 1.5
6	5 [0]	2.40 [+1]	96.3 ± 3.4	20.0 ± 1.2
7	7 [+1]	0.80 [−1]	86.6 ± 3.0	53.8 ± 2.5
8	7 [+1]	1.60 [0]	95.7 ± 3.1	29.9 ± 1.5
9	7 [+1]	2.50 [+1]	96.8 ± 3.2	20.1 ± 1.2

Note: R: malachite green removal percentage; q: biosorption capacity. [a]Mean ± standard deviation ($n = 3$).

results are positive since they exhibit the versatility of the system under study in terms of pH experimental conditions. On the other hand, it was also observed that the biosorption capacities change as the biosorbent dose varies, increasing the response as the biosorbent dose decreases, which is convenient due to the highest biosorption capacity that was obtained using a minimum stalk amount.

The significance of the variables on the percentage of removal and the biosorption capacity was evaluated using the Pareto diagrams; the graphs can be seen in Supplementary Figure 1. Analysis of variance (ANOVA) was used to verify the statistical significance of the biosorbent dose and pH on the removal and biosorption capacity responses. The analysis showed that both variables and their linear, quadratic, and interaction effects were significant ($p = 0.05$). Statistical polynomial quadratic models showed the removal percentage (Equation (4)) and the biosorption capacity (Equation (5)) as a function of the biosorbent dose (x_1) and the pH (x_2).

$$R = 95.29 + 1.06x_1^2 - 1.63x_2^2 + 5.36x_1 - 2.94x_2 - 0.50x_1x_2, \quad (4)$$

$$q = 30.08 + 0.89x_1^2 - 0.99x_2^2 - 16.83x_1 + 7.50x_2 - 0.66x_1x_2. \quad (5)$$

An ANOVA and a Fisher test were performed to verify the significance and predictivity of the statistical models, respectively. The determination coefficient values for both responses were high ($R^2 = 0.968$ and 0.998), which indicates that the models were significant and adequately described the relation between the variables. The calculated F values ($F_{cal} = 74.74$ and 1248.58) were found to be above the Fisher standard value ($F_{std} = 3.106$), indicating that the quadratic models were predictive.

From the statistical models, response surface graphs were made for both the removal percentage and the biosorption capacity. Figure 4(a) shows the response surface graph to represent the removal percentage as a function of the independent variables. It can be seen that an increase in the biosorbent dose caused an increase in the removal percentage. Regarding the behavior as a function of pH, a slight influence on the response was observed from pH 5, which could be explained through the pH of the medium, since the working pH value is higher than the pH_{pzc} of the biosorbent. In this way, the surface of the stalk is negatively charged, thus being able to interact with the positively charged dye molecules [29]. Figure 4(b) shows that the biosorption capacity decreased when the biosorbent dose is increased. Based on the results obtained in the modeling and the statistical optimization of variables, the optimal experimental conditions were defined at pH 5 and a biosorbent dose of $0.80\,g\,L^{-1}$; under these conditions, it was possible to remove 87.7% of MG and reach a biosorption capacity of $54.8\,mg\,g^{-1}$.

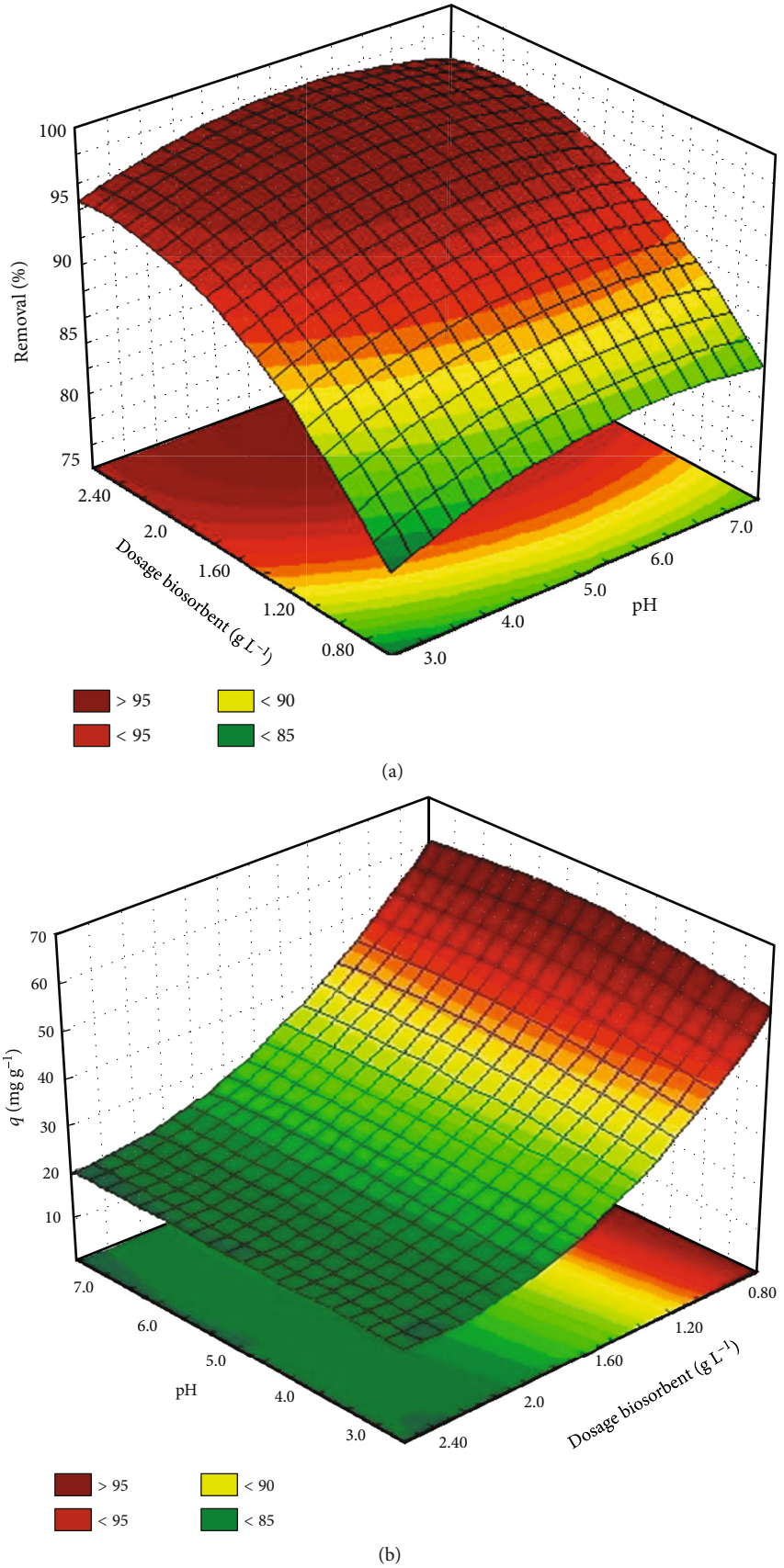

Figure 4: Response surfaces of MG for removal percentage (a) and biosorption capacity (b) using grape stalk as biosorbent.

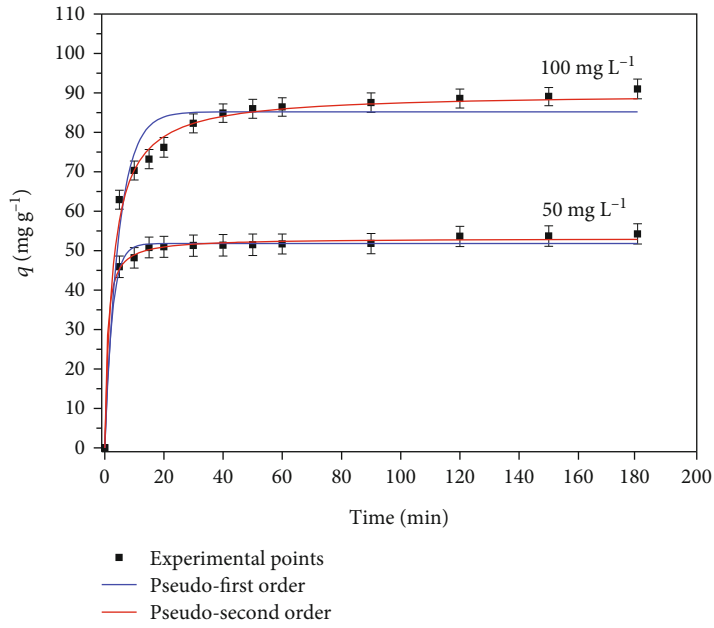

Figure 5: Biosorption kinetic curve using 50 mg L^{-1} and 100 mg L^{-1} as initial concentrations of MG (biosorbent dose: 0.80 g L^{-1}, pH 5, and T = 298 K).

3.3. Biosorption Kinetic Curves and Modeling. Figure 5 shows the MG adsorption kinetics. It is possible to observe that, during the first 5 min of the removal process, there was a marked increase in the biosorption capacity. Equilibrium time was established at approximately 120 min. An increase in the biosorption capacity could also be seen when the dye concentration increased; this is attributed to the fact that the initial MG concentration acted as a driving force, since it would allow overcoming the resistance to mass transfer between the aqueous and solid phases [40].

In order to deeply understand the MG biosorption process on grape stems, PFO and PSO kinetic models were tested to adjust the obtained experimental kinetic data. Table 2 shows the kinetic parameters for the proposed models. From the analysis of the results, the PSO model showed a better fit with the experimental data because it presented a high R^2 and lower ARE than those obtained for the PFO model. It was observed that the highest value of q_2 was reached at an MG concentration of 100 mg L^{-1}. This maximum amount of adsorbed MG predicted by the models was comparable with that obtained experimentally, which suggests that they can be used for the reliable analysis of this system.

The value of the initial biosorption rate (h_0) decreased for higher dye concentrations, making the biosorption faster when the initial dye concentration was 50 mg L^{-1}. This situation may be due to a decrease in the active biosorption sites available on the surface of the biosorbent [41].

3.4. Equilibrium Study and Theoretical Modeling. The biosorption isotherm study was performed at four temperatures (298, 308, 318, and 328 K). Figure 6 shows the isotherms at all tested temperatures. It can be seen that the increase in temperature generated a decrease in the biosorption capacity; this behavior is associated with an exothermic process and means considerable energy savings in the process, since it must be developed at room temperature to achieve the highest response.

Table 2: Kinetic parameters for MG adsorption by grape stalk.

Model	Initial concentration of MG	
	50 mg L^{-1}	100 mg L^{-1}
Pseudofirst order		
k_1 (min^{-1})	0.407	0.209
q_1 (mg g^{-1})	51.8	85.2
R^2	0.995	0.979
ARE (%)	1.99	4.85
Pseudosecond order		
k_2 (g mg^{-1} min^{-1})	0.022	0.004
q_2 (mg g^{-1})	53.1	89.9
h_0 (mg g^{-1} min^{-1})	62.0	32.3
R^2	0.998	0.996
ARE (%)	1.23	1.72
q_{exp} (mg g^{-1})	54.2	91.0

Two isothermal models (Langmuir and Freundlich) were used to correlate the experimental equilibrium data. The selection of the models was based on the convex shape of the isotherms obtained, which agree with type I isotherms and can be adjusted to these models [42]. Table 3 shows the biosorption isotherm parameters obtained at all temperatures. It can be seen that the Langmuir model presented the highest values of R^2 and the lowest values of ARE at all studied temperatures. Therefore, the Langmuir isotherm model was selected as the most appropriate because it better

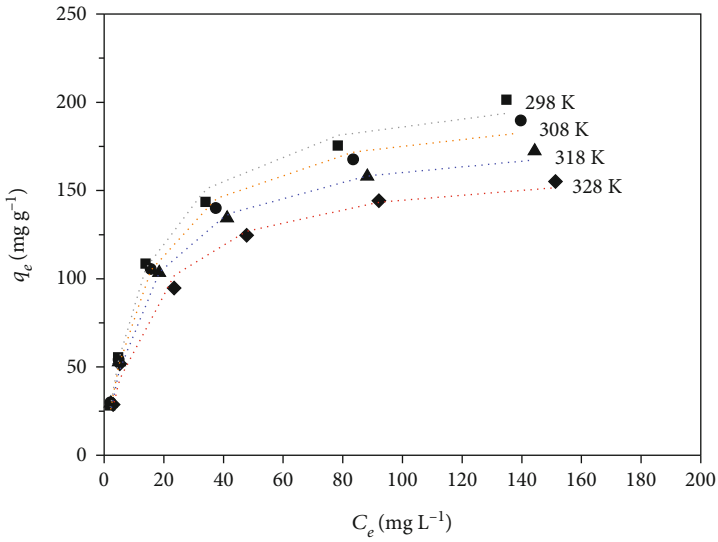

Figure 6: Isotherm curves of MG adsorption by grape stalk (biosorbent dose: 0.80 g L^{-1} and pH 5).

Table 3: Parameters of the equilibrium models tested for the biosorption of MG on grape stalks.

Model	Temperature (K)			
	298	308	318	328
Langmuir				
q_m (mg g^{-1})	214.2	201.6	183.9	166.6
k_L (L mg^{-1})	0.070	0.069	0.070	0.067
R^2	0.997	0.998	0.998	0.996
ARE (%)	3.45	4.10	3.78	4.55
Freundlich				
k_F ((mg g^{-1}) (mg L^{-1})$^{-1/nF}$)	36.9	35.8	34.7	30.5
$1/n_F$	2.85	2.88	3.03	2.96
R^2	0.986	0.987	0.985	0.986
ARE (%)	16.3	14.0	13.8	11.8

described the MG biosorption process at equilibrium, which allows assuming a homogeneous distribution of adsorption sites and the formation of a monolayer dye on the biosorbent surface [43, 44].

The maximum biosorption capacity decreased when increasing temperature, which indicates that the biosorption process is favored at room temperature; the maximum value was 214.2 mg g^{-1}. These results are similar to those obtained in other studies involving the MG adsorption on different biosorbent materials, such as agricultural residues [45], sludge [46], and leaves [47].

3.5. Biosorption Thermodynamic Behavior. Table 4 shows the thermodynamic parameters obtained from the grape stalk-MG biosorption process. Negative values of ΔG° can be observed, indicating that the biosorption process was favorable and spontaneous at all studied temperatures. The negative value of ΔH° showed the exothermic nature of the biosorption process. The magnitude of the standard enthalpy changes was consistent with a process of physical adsorption type. These results are in agreement with those obtained in the FTIR spectra, so it could be thought that the interaction between the functional groups present on the surface of the biosorbent and the dye molecule would occur through weak interactions that respond to a physical adsorption process. Finally, ΔS° presented a positive value, which suggests a good affinity of the dye molecules towards

Table 4: Thermodynamic parameters for MG adsorption using stalks.

Temperature (K)	ΔG° (kJ Mol^{-1})	ΔH° (kJ Mol^{-1})	ΔS° (kJ Mol^{-1} K^{-1})
298	-23.80	-8.09	0.05
308	-24.40		
318	-24.98		
328	-25.36		

Table 5: Comparison of MG removal using different biosorbents previously reported.

Biosorbent	Optimum working conditions				R (%)[a]	q_m (mg g^{-1})[b]	Reference
	pH	Biosorbent dosage (g L^{-1})	Contact time (min)	Temperature (K)			
Garlic root biomass	8.00	1.60	120	288	55.8	172	[40]
Pomegranate peel	6.00	0.10[c]	90	323	99.1	31.4	[49]
Sargassum swartzii macroalgae	10.0	0.10[c]	180	303	n.r.[d]	76.9	[50]
Limonia acidissima (wood apple)	7.50	0.05	210	299	98.9	35.8	[51]
Potato peel	4.00	0.25[c]	n.r.	318	n.r.	35.6	[52]
Rice husks	7.00	0.10[c]	40	296	95.7	6.50	[53]
Luffa acutangula peel	4.00	8.00	180	303	92.1	69.6	[54]
Grape stalk	5.00	0.80	120	298	87.7	214	This work

[a]R: MG removal percentage. [b]q: biosorption capacity. [c]Biosorbent dosage expressed in grams. [d]Value not reported.

Table 6: Percentages of MG removal in samples of natural waters and effluents (95% confidence interval; $n = 6$).

Sample	MG		Removal (%)
	Aggregate (mg L^{-1})	Found in aqueous phase (mg L^{-1})	
Seawater	0	n.d.[*]	—
	25	6.3 ± 0.7	74.8
	50	20.1 ± 2.1	59.8
River water	0	n.d.	—
	25	6.7 ± 0.7	72.8
	50	16.7 ± 1.8	66.4
Dam water	0	n.d.	—
	25	6.0 ± 0.6	75.9
	50	14.2 ± 1.6	71.6
Well water	0	n.d.	—
	25	6.3 ± 0.7	74.8
	50	30.4 ± 2.3	58.2
Agricultural effluent	0	n.d.	—
	25	2.9 ± 0.3	88.2
	50	8.9 ± 2.1	82.0
Simulated textile effluent	0	n.d.	—
	25	1.9 ± 0.2	92.5
	50	5.7 ± 2.1	88.6
Real textile effluent	0	4.6 ± 0.5	84.3
	25	7.3 ± 0.7	70.8
	50	16.7 ± 1.5	66.6

[*]n.d.: not detected.

the biosorbent and showed an increase in the randomness of the molecules in the solid-liquid interface during the biosorption process [29, 44, 48].

3.6. Comparative Study of the Biosorption Efficiency. The biosorption efficiency obtained in this research work was evaluated by conducting a comparative study of different biosorbent-MG systems previously reported in the literature. The maximum biosorption capacity obtained in the present work was higher than those reported using other biosorbent materials, which suggests that stalks are promising materials for MG removal. Table 5 shows that other works used higher biosorbent doses to remove similar MG concentrations in comparison with our contribution. The stalk is an economic

biomaterial that was used at very low doses for the removal of the pollutant at the assayed concentrations.

3.7. Grape Stalk Application for MG Removal in Real Samples. The stalk biosorbent was applied to real samples of natural water from various sources, to textile and agricultural effluents, and to a synthetic effluent. The results can be seen in Table 6. The removal percentages were high in the natural water samples, which indicated that the stalk was efficient as a biosorbent for the MG removal from complex matrices. In the case of real effluents, removal percentages above 60.0% were recorded, which is extremely positive considering that an inexpensive and easily accessible biosorbent material is being used. It should be noted that the removal percentage in the real textile effluent sample without added MG was 84.3%, which demonstrated the efficiency of the stalk as a biosorbent for the textile wastewater treatment.

4. Conclusions

Grape stalk was studied as a biosorbent for the removal of MG from natural water samples and industrial effluents. Under optimal conditions, the dye removal was 87.7%. The PSO kinetic model was the best to fit the experimental data. The Langmuir isotherm model adequately represented the biosorption process, reaching a maximum biosorption capacity of 214.2 $mg\,g^{-1}$. From thermodynamic studies, it was possible to establish that the MG removal using grape stalk was favorable, occurs spontaneously, was exothermic, and was associated to physical interaction forces, which implies an advantage because it does not require the addition of energy, which indicates greater profitability in a possible industrial application. The biosorbent was applied to real samples, obtaining MG removal percentages higher than 58.0% for natural waters and higher than 82.0% for textile effluents. Therefore, grape stalk is an alternative and environmentally friendly material for the treatment of wastewater.

Data Availability

All data have been included in the manuscript and in the supplementary files.

Conflicts of Interest

The authors declare that there is no conflict of interest regarding the publication of this paper.

Acknowledgments

The authors would like to thank the Consejo Nacional de Investigaciones Científicas y Técnicas (CONICET-PIBAA 1208, Director: Leticia B. Escudero), the Universidad Nacional de Cuyo (Project M015-T1, Director: Leticia B. Escudero), the Organisation for the Prohibition of Chemical Weapons (OPCW Project 2020–2023, Director: Leticia B. Escudero), the European Union (EU), and the Organización de Estados Iberoamericanos (OEI) (Project in the frame of IBERBIOMASA network, Director: Adrián Bonilla Petriciolet) for the financial support.

Supplementary Materials

Supplementary 1. Supplementary Material 1: kinetic and equilibrium models utilized.

Supplementary 2. Supplementary Material 2: equations of thermodynamic parameters.

Supplementary 3. Supplementary Material 3: equations used to calculate the coefficient of determination (R^2) and the mean relative error (ARE).

Supplementary 4. Supplementary Figure 1: the Pareto diagrams of the removal of malachite green (a) and biosorption capacity (b).

References

[1] A. Choudhury, "Textile effluents: types and prominent hazards," in *Handbook of Textile Effluent Remediation*, pp. 1–39, Jenny Stanford Publishing, Standford, 2018.

[2] S. Mani, P. Chowdhary, and R. N. Bharagava, "Textile wastewater dyes: toxicity profile and treatment approaches," in *Emerging and Eco-Friendly Approaches for Waste Management*, pp. 219–244, Springer, 2019.

[3] S. Bhatia and S. Devraj, *Pollution Control in Textile Industry*, WPI Publishing, 2017.

[4] M. Ilyas, W. Ahmad, H. Khan, S. Yousaf, M. Yasir, and A. Khan, "Environmental and health impacts of industrial wastewater effluents in Pakistan: a review," *Reviews on Environmental Health*, vol. 34, no. 2, pp. 171–186, 2019.

[5] S. Devraj, "Textile industry and its impact on environment," in *Pollution Control in Textile Industry*, pp. 22–39, WPI Publishing, 2017.

[6] M. Shabbir and M. Naim, *Introduction to Textiles and the Environment in Textiles and Clothing Environmental Concerns and Solutions*, John Wiley & Sons, 2019.

[7] I. Dahlan and N. W. Ling, "Adsorption of acid violet 7 (AV7) dye using RHA-CFA adsorbent: modeling, process analysis, and optimization," *Separation Science Technology*, vol. 56, no. 1, pp. 54–67, 2021.

[8] Z. Chen, H. Deng, C. Chen, Y. Yang, and H. Xu, "Biosorption of malachite green from aqueous solutions by Pleurotus ostreatus using Taguchi method," *Journal of Environmental Health Science Engineering*, vol. 12, no. 1, pp. 1–10, 2014.

[9] S. Banerjee, G. C. Sharma, R. K. Gautam, M. C. Chattopadhyaya, S. N. Upadhyay, and Y. C. Sharma, "Removal of malachite green, a hazardous dye from aqueous solutions using *Avena sativa* (oat) hull as a potential adsorbent," *Journal of Molecular Liquids*, vol. 213, pp. 162–172, 2016.

[10] J. C. Hashimoto, J. A. R. Paschoal, J. F. de Queiroz, and F. G. R. Reyes, "Considerations on the use of malachite green in aquaculture and analytical aspects of determining the residues in fish: a review," *Journal of Aquatic Food Product Technology*, vol. 20, no. 3, pp. 273–294, 2011.

[11] S. Srivastava, R. Sinha, and D. Roy, "Toxicological effects of malachite green," *Aquatic Toxicology*, vol. 66, no. 3, pp. 319–329, 2004.

[12] K. Tewari, G. Singhal, and R. K. Arya, "Adsorption removal of malachite green dye from aqueous solution," *Reviews in Chemical Engineering*, vol. 34, no. 3, pp. 427–453, 2018.

[13] W. Li, B. Mu, and Y. Yang, "Feasibility of industrial-scale treatment of dye wastewater via bio-adsorption technology," *Bioresource Technology*, vol. 277, pp. 157–170, 2019.

[14] P. Matpang, M. Sriuttha, and N. Piwpuan, "Effects of malachite green on growth and tissue accumulation in pak choy (*Brassica chinensis* Tsen & Lee)," *Agriculture and Natural Resources*, vol. 51, no. 2, pp. 96–102, 2017.

[15] Y. Zhou, J. Lu, Y. Zhou, and Y. Liu, "Recent advances for dyes removal using novel adsorbents: a review," *Environmental Pollution*, vol. 252, no. Part A, pp. 352–365, 2019.

[16] D. H. A. Sudarni, U. O. Aigbe, K. E. Ukhurebor et al., "Malachite green removal by activated potassium hydroxide clove leaf agrowaste biosorbent: characterization, kinetic, isotherm, and thermodynamic studies," *Adsorption Science Technology*, vol. 2021, pp. 1–15, 2021.

[17] S. Samsami, M. Mohamadizaniani, M. H. Sarrafzadeh, E. R. Rene, and M. Firoozbahr, "Recent advances in the treatment of dye-containing wastewater from textile industries: overview and perspectives," *Process Safety Environmental Protection*, vol. 143, pp. 138–163, 2020.

[18] E. Rápó and S. Tonk, "Factors affecting synthetic dye adsorption; desorption studies: a review of results from the last five years (2017–2021)," *Molecules*, vol. 26, no. 17, p. 5419, 2021.

[19] S. Kiran, S. Adeel, S. Nosheen, A. Hassan, M. Usman, and M. A. Rafique, "Recent trends in textile effluent treatments: a review," in *Advanced Materials for Wastewater Treatment*, S. Ul-Islam, Ed., pp. 29–49, Scrivener Publishing LLC, 2017.

[20] Aruna, N. Bagotia, A. K. Sharma, and S. Kumar, "A review on modified sugarcane bagasse biosorbent for removal of dyes," *Chemosphere*, vol. 268, article 129309, 2021.

[21] I. Dahlan and S. Ismail, "Physical characterization of prepared and spent CFA/PFA/RHA sorbents in removing heavy metals and dyes," *Journal of Environmental Science and Technology*, vol. 5, no. 3, pp. 177–183, 2012.

[22] S. Rajendran, A. K. Priya, P. Senthil Kumar et al., "A critical and recent developments on adsorption technique for removal of heavy metals from wastewater-a review," *Chemosphere*, vol. 303, Part 2, article 135146, 2022.

[23] I. Dahlan, O. H. Keat, H. A. Aziz, and Y. T. Hung, "Synthesis and characterization of MOF-5 incorporated waste-derived siliceous materials for the removal of malachite green dye from aqueous solution," *Sustainable Chemistry Pharmacy*, vol. 31, article 100954, 2023.

[24] L. Bulgariu, L. B. Escudero, O. S. Bello et al., "The utilization of leaf-based adsorbents for dyes removal: a review," *Journal of Molecular Liquids*, vol. 276, pp. 728–747, 2019.

[25] D. T. C. Nguyen, T. V. Tran, P. S. Kumar, A. T. M. Din, A. A. Jalil, and D. V. N. Vo, "Invasive plants as biosorbents for environmental remediation: a review," *Environmental Chemistry Letters*, vol. 20, no. 2, pp. 1421–1451, 2022.

[26] E. S. Lemos, E. B. Ingrassia, and L. B. Escudero, "Recent Literature on Biosorption as a Sustainable Environmental Technology to Remove Pollutants," in *Biotechnology for Toxicity Remediation Environmental Sustainability*, R. S. K. M. Gothandam, S. Ranjan, and N. Dasgupta, Eds., Taylor and Francis Group: CRC Press, 2023.

[27] S. Haydar, M. Farooq, and S. Gull, "Use of grape vine bark as an effective biosorbent for the removal of heavy metals (copper and lead) from aqueous solutions," *Desalination Water Treatment*, vol. 183, pp. 307–314, 2020.

[28] L. B. Escudero, G. Vanni, F. A. Duarte, T. Segger, and G. L. Dotto, "Biosorption of silver from aqueous solutions using wine industry wastes," *Chemical Engineering Communications*, vol. 205, no. 3, pp. 325–337, 2018.

[29] L. B. Escudero, E. Agostini, and G. L. Dotto, "Application of tobacco hairy roots for the removal of malachite green from aqueous solutions: experimental design, kinetic, equilibrium, and thermodynamic studies," *Chemical Engineering Communications*, vol. 205, no. 1, pp. 122–133, 2018.

[30] M. R. Kumar, P. King, Z. Wolde, and M. Mulu, "Application of optimization response surface for the biosorption of crystal violet dye from textile wastewater onto *Clerodendrum fragrans* leaves," *Biomass Conversion Biorefinery*, pp. 1–16, 2022.

[31] I. Langmuir, "The adsorption of gases on plane surfaces of glass, mica and platinum," *Journal of the American Chemical Society*, vol. 40, no. 9, pp. 1361–1403, 1918.

[32] H. Freundlich, "Over the adsorption in solution," *The Journal of Physical Chemistry*, vol. 57, no. 385471, pp. 1100–1107, 1906.

[33] G. Brião, S. L. Jahn, E. L. Foletto, and G. L. Dotto, "Adsorption of crystal violet dye onto a mesoporous ZSM-5 zeolite synthetized using chitin as template," *Journal of Colloid Interface Science*, vol. 508, pp. 313–322, 2017.

[34] A. L. D. da Rosa, E. Carissimi, G. L. Dotto, H. Sander, and L. A. Feris, "Biosorption of rhodamine B dye from dyeing stones effluents using the green microalgae *Chlorella pyrenoidosa*," *Journal of Cleaner Production*, vol. 198, pp. 1302–1310, 2018.

[35] M. J. Firdhouse and P. Lalitha, "Nanosilver-decorated nanographene and their adsorption performance in waste water treatment," *Bioresources and Bioprocessing*, vol. 3, no. 1, pp. 1–15, 2016.

[36] R. Portinho, O. Zanella, and L. A. Féris, "Grape stalk application for caffeine removal through adsorption," *Journal of Environmental Management*, vol. 202, Part 1, pp. 178–187, 2017.

[37] J. Benvenuti, A. Giraldi Fisch, J. H. Zimnoch dos Santos, and M. Gutterres, "Hybrid sol–gel silica adsorbent material based on grape stalk applied to cationic dye removal," *Environmental Progress Sustainable Energy*, vol. 39, no. 4, article e13398, 2020.

[38] S. O. Prozil, D. V. Evtuguin, and L. P. C. Lopes, "Chemical composition of grape stalks of *Vitis vinifera* L. from red grape pomaces," *Industrial Crops and Products*, vol. 35, no. 1, pp. 178–184, 2012.

[39] I. Villaescusa, N. Fiol, M:. Martínez, N. Miralles, J. Poch, and J. Serarols, "Removal of copper and nickel ions from aqueous solutions by grape stalks wastes," *Water Research*, vol. 38, no. 4, pp. 992–1002, 2004.

[40] H. Ren, R. Zhang, Q. Wang, H. Pan, and Y. Wang, "Garlic root biomass as novel biosorbents for malachite green removal: parameter optimization, process kinetics and toxicity test," *Chemical Research in Chinese Universities*, vol. 32, no. 4, pp. 647–654, 2016.

[41] L. Ma, C. Jiang, Z. Lin, and Z. Zou, "Microwave-hydrothermal treated grape peel as an efficient biosorbent for methylene blue removal," *International Journal of Environmental Research Public Health*, vol. 15, no. 2, p. 239, 2018.

[42] G. Blázquez, M. Calero, F. Hernáinz, G. Tenorio, and M. A. Martín-Lara, "Equilibrium biosorption of lead(II) from

aqueous solutions by solid waste from olive-oil production," *Chemical Engineering Journal*, vol. 160, no. 2, pp. 615–622, 2010.

[43] D. Shahbazi, S. Mousavi, and D. Nayeri, "Low-cost activated carbon: characterization, decolorization, modeling, optimization and kinetics," *International Journal of Environmental Science Technology*, vol. 17, no. 9, pp. 3935–3946, 2020.

[44] X.-F. Sun, S. G. Wang, X. W. Liu et al., "Biosorption of malachite green from aqueous solutions onto aerobic granules: kinetic and equilibrium studies," *Bioresource Technology*, vol. 99, no. 9, pp. 3475–3483, 2008.

[45] P. Saha, S. Chowdhury, S. Gupta, I. Kumar, and R. Kumar, "Assessment on the removal of malachite green using tamarind fruit shell as biosorbent," *Water*, vol. 38, no. 5-6, pp. 437–445, 2010.

[46] W. Cheng, S. G. Wang, L. Lu et al., "Removal of malachite green (MG) from aqueous solutions by native and heat-treated anaerobic granular sludge," *Biochemical Engineering Journal*, vol. 39, no. 3, pp. 538–546, 2008.

[47] P. Pallavi, P. King, and Y. P. Kumar, "Use of plant biomass for removal of malachite green from aqueous solution and optimization using central composite design (CCD)," *Rasāyan Journal of Chemistry*, vol. 11, no. 1, pp. 203–218, 2018.

[48] L. Wang and J. Li, "Removal of methylene blue from aqueous solution by adsorption onto crofton weed stalk," *BioResources*, vol. 8, no. 2, pp. 2521–2536, 2013.

[49] F. Gündüz and B. Bayrak, "Biosorption of malachite green from an aqueous solution using pomegranate peel: equilibrium modelling, kinetic and thermodynamic studies," *Journal of Molecular Liquids*, vol. 243, pp. 790–798, 2017.

[50] M. Jerold and V. Sivasubramanian, "Biosorption of malachite green from aqueous solution using brown marine macro algae *Sargassum swartzii*," *Desalination Water Treatment*, vol. 57, no. 52, pp. 25288–25300, 2016.

[51] A. S. Sartape, A. M. Mandhare, V. V. Jadhav, P. D. Raut, M. A. Anuse, and S. S. Kolekar, "Removal of malachite green dye from aqueous solution with adsorption technique using *Limonia acidissima* (wood apple) shell as low cost adsorbent," *Arabian Journal of Chemistry*, vol. 10, pp. S3229–S3238, 2017.

[52] E.-K. Guechi and O. Hamdaoui, "Sorption of malachite green from aqueous solution by potato peel: kinetics and equilibrium modeling using non-linear analysis method," *Arabian Journal of Chemistry*, vol. 9, pp. S416–S424, 2016.

[53] V. Muinde, J. M. Onyari, B. Wamalwa, J. Wabomba, and R. M. Nthumbi, "Adsorption of malachite green from aqueous solutions onto rice husks: kinetic and equilibrium studies," *Journal of Environmental Protection*, vol. 8, no. 3, pp. 215–230, 2017.

[54] H. W. Ng, L. Y. Lee, W. L. Chan, S. Gan, and N. Chemmangattuvalappil, "Luffa acutangulapeel as an effective natural biosorbent for malachite green removal in aqueous media: equilibrium, kinetic and thermodynamic investigations," *Desalination Water Treatment*, vol. 57, no. 16, pp. 7302–7311, 2016.